



Highly sensitive torsion sensor with femtosecond laser-induced low birefringence single-mode fiber based Sagnac interferometer

BO HUANG AND XUEWEN SHU*

Wuhan National Laboratory for Optoelectronics & Optical and Electronic Information, Huazhong University of Science and Technology, Wuhan 430074, China
*xshu@hust.edu.cn

Abstract: A highly sensitive optical fiber torsion sensor with femtosecond laser-induced low birefringence SMF-based Sagnac interferometer (SI) is proposed and experimentally demonstrated in this paper. A straight-line waveguide positioned horizontally with respect to the fiber core is inscribed by the femtosecond laser in the cladding of the SMF, which leads to the asymmetry stress distribution in the SMF, and then gives rise to the low birefringence in the SMF. Compared with most of the previous reported SI based torsion sensors, there is no splicing joint in the femtosecond laser-induced low birefringence SMF-based SI, which lowers the transmission loss and makes the SI based torsion sensor more robust simultaneously. The experiment result shows that the proposed torsion sensor exhibits a torsion sensitivity of up to 3.2562 nm/degree, with the high torsion resolution of 0.003 degree. In contrast, the temperature cross-sensitivity and strain cross-sensitivity of the proposed torsion sensor are low, to -0.000055 degree/ $^{\circ}\text{C}$ and 0.000013 degree/ μe , respectively, thus overcoming the cross-sensitivity problem resulting from temperature and strain. Moreover, theoretical analysis are carried out to compare with the experimental results to demonstrate the feasibility and good consistency.

© 2018 Optical Society of America under the terms of the [OSA Open Access Publishing Agreement](#)

OCIS codes: (060.2370) Fiber optics sensors; (320.7140) Ultrafast processes in fibers; (060.2420) Fibers, polarization-maintaining.

References and links

1. P. L. Fulmek, F. Wandling, W. Zdiarsky, G. Brasseur, and S. P. Cermak, "Capacitive sensor for relative angle measurement," *IEEE Trans. Instrum. Meas.* **51**(6), 1145–1149 (2002).
2. D. Vischer and O. Khatib, "Design and development of high-performance torque controlled joints," *IEEE Trans. Robot. Autom.* **11**(4), 537–544 (1995).
3. D. E. Ceballos-Herrera, I. Torres-Gomez, A. Martinez-Rios, L. Garcia, and J. J. Sanchez-Mondragon, "Torsion sensing characteristics of mechanically induced long-period holey fiber gratings," *IEEE Sens. J.* **10**(7), 1200–1205 (2010).
4. R. Gao, Y. Jiang, and L. Jiang, "Multi-phase-shifted helical long period fiber grating based temperature-insensitive optical twist sensor," *Opt. Express* **22**(13), 15697–15709 (2014).
5. L. Xian, P. Wang, and H. Li, "Power-interrogated and simultaneous measurement of temperature and torsion using paired helical long-period fiber gratings with opposite helicities," *Opt. Express* **22**(17), 20260–20267 (2014).
6. J. Wo, M. Jiang, M. Malnou, Q. Sun, J. Zhang, P. P. Shum, and D. Liu, "Twist sensor based on axial strain insensitive distributed Bragg reflector fiber laser," *Opt. Express* **20**(3), 2844–2850 (2012).
7. F. Yang, Z. Fang, Z. Pan, Q. Ye, H. Cai, and R. Qu, "Orthogonal polarization mode coupling for pure twisted polarization maintaining fiber Bragg gratings," *Opt. Express* **20**(27), 28839–28845 (2012).
8. W. Yiping, M. Wang, and X. Huang, "In fiber Bragg grating twist sensor based on analysis of polarization dependent loss," *Opt. Express* **21**(10), 11913–11920 (2013).
9. X. Chen, K. Zhou, L. Zhang, and I. Bennion, "In-fiber twist sensor based on a fiber Bragg grating with 81° tilted structure," *IEEE Photonics Technol. Lett.* **18**(24), 2596–2598 (2006).
10. B. Huang and X. Shu, "Ultra-compact strain- and temperature-insensitive torsion sensor based on a line-by-line inscribed phase-shifted FBG," *Opt. Express* **24**(16), 17670–17679 (2016).
11. B. Song, Y. Miao, W. Lin, H. Zhang, J. Wu, and B. Liu, "Multi-mode interferometer-based twist sensor with low temperature sensitivity employing square coreless fibers," *Opt. Express* **21**(22), 26806–26811 (2013).
12. L. Chen, W. G. Zhang, L. Wang, H. Zhang, J. Sieg, Q. Zhou, L. Y. Zhang, B. Wang, and T. Y. Yan, "In-fiber torsion sensor based on dual polarized Mach-Zehnder interference," *Opt. Express* **22**(26), 31654–31664 (2014).
13. L. A. Fernandes, J. R. Grenier, J. S. Aitchison, and P. R. Herman, "Fiber optic stress-independent helical torsion sensor," *Opt. Lett.* **40**(4), 657–660 (2015).

14. Q. Zhou, W. Zhang, L. Chen, T. Yan, L. Zhang, L. Wang, and B. Wang, "Fiber torsion sensor based on a twist taper in polarization-maintaining fiber," *Opt. Express* **23**(18), 23877–23886 (2015).
15. B. Huang, X. Shu, and Y. Du, "Intensity modulated torsion sensor based on optical fiber reflective Lyot filter," *Opt. Express* **25**(5), 5081–5090 (2017).
16. B. Huang and X. Shu, "Highly Sensitive Twist Sensor Based on Temperature- and Strain-Independent Fiber Lyot Filter," *J. Lightwave Technol.* **35**(10), 2026–2031 (2017).
17. O. Frazão, S. O. Silva, J. M. Baptista, J. L. Santos, G. Statkiewicz-Barabach, W. Urbanczyk, and J. Wojcik, "Simultaneous measurement of multiparameters using a Sagnac interferometer with polarization maintaining side-hole fiber," *Appl. Opt.* **47**(27), 4841–4848 (2008).
18. O. Frazão, R. M. Silva, J. Kobelke, and K. Schuster, "Temperature- and strain-independent torsion sensor using a fiber loop mirror based on suspended twin-core fiber," *Opt. Lett.* **35**(16), 2777–2779 (2010).
19. W. Chen, S. Lou, L. Wang, H. Zou, W. Lu, and S. Jian, "Highly sensitive torsion sensor based on Sagnac interferometer using side-leakage photonic crystal fiber," *IEEE Photonics Technol. Lett.* **23**(21), 1639–1641 (2011).
20. H. Kim, T. Kim, B. Kim, and Y. Chung, "Temperature-insensitive torsion sensor with enhanced sensitivity by use of a highly birefringent photonic crystal fiber," *IEEE Photonics Technol. Lett.* **22**(20), 1539–1541 (2010).
21. P. Zu, C. Chan, Y. Jin, T. Gong, Y. Zhang, L. Chen, and X. Dong, "A temperature-insensitive twist sensor by using low-birefringence photonic-crystal-fiber-based Sagnac interferometer," *IEEE Photonics Technol. Lett.* **23**(13), 920–922 (2011).
22. K. Naeem, B. H. Kim, B. Kim, and Y. Chung, "Simultaneous multi-parameter measurement using Sagnac loop hybrid interferometer based on a highly birefringent photonic crystal fiber with two asymmetric cores," *Opt. Express* **23**(3), 3589–3601 (2015).
23. B. Song, H. Zhang, Y. Miao, W. Lin, J. Wu, H. Liu, D. Yan, and B. Liu, "Highly sensitive twist sensor employing Sagnac interferometer based on PM-elliptical core fibers," *Opt. Express* **23**(12), 15372–15379 (2015).
24. Y. Chen, Y. Semenova, G. Farrell, F. Xu, and Y. Lu, "A compact Sagnac loop based on a microfiber coupler for twist sensing," *IEEE Photonics Technol. Lett.* **27**(24), 2579–2582 (2015).
25. L. A. Fernandes, J. R. Grenier, P. V. S. Marques, J. S. Aitchison, and P. R. Herman, "Strong birefringence tuning of optical waveguides with femtosecond laser irradiation of bulk fused silica and single mode fibers," *J. Lightwave Technol.* **31**(22), 3563–3569 (2013).
26. D. Grobncic, S. J. Mihailov, and C. W. Smelser, "Localized High Birefringence Induced in SMF-28 Fiber by Femtosecond IR Laser Exposure of the Cladding," *J. Lightwave Technol.* **25**(8), 1996–2001 (2007).
27. R. Ulrich and A. Simon, "Polarization optics of twisted single-mode fibers," *Appl. Opt.* **18**(13), 2241–2251 (1979).
28. A. J. Barlow, J. J. Ramkov-Hansen, and D. N. Payne, "Birefringence and polarization mode-dispersion in spun single-mode fibers," *Appl. Opt.* **20**(17), 2962–2968 (1981).

1. Introduction

Torsion sensors have been receiving extensive interest in the area of the modern smart structure monitoring because torsion is an important mechanical parameter that reflects the stress state and internal injury of the monitored structure. And accordingly, numerous torsion sensors have been proposed based on various solutions. Conventional torsion sensors are usually based on electromagnetic phenomena [1] and electrical methods [2]. For the electromagnetic phenomena based torsion sensors, the bulky heavy structure and the complicated manufacturing limit the practical application. For the electrical methods based torsion sensors, they suffer large cross-sensitivities from the electrical noise and temperature. Optical fiber torsion sensors, by contrast, are in general inherently insulation, compact footprint, lowered weight, and electromagnetic interference- and hazard-free, and therefore superior in applications requiring operation within the harsh environment.

Fiber optic torsion sensors, as a very promising technique, have gained a lot of attentions and long been researched. Nowadays, various types of optical fiber torsion sensor based on various types of fiber components have been developed and widely used [3–21]. In general, according to the fiber optic device configuration, fiber optic torsion sensors can be classed into two main principal categories: sensors based on fiber gratings [3–10] and sensors based on fiber interferometers [11–21]. In the fiber grating configuration, the fiber grating is used as the sensor head. Up to now, a considerable amount of fiber gratings have been employed to construct fiber optic torsion sensors, such as long period gratings (LPGs) [3–5], fiber Bragg gratings (FBGs) [6–8] and tilted FBGs (TFBGs) [9]. And more recently, a phase shifted FBG (PSFBG) based fiber optic torsion sensor has been proposed [10]. Meanwhile, the other common fiber optic torsion sensor, namely, the fiber interferometer based torsion sensors, have attracted increasing research interests due to the fast response, easy fabrication and great

interference fringes, which could be fulfilled by Mach Zehnder Interference (MZI) [11–16], and Sagnac interference (SI) [17–21]. In particular, the SI based fiber torsion sensors are attractive owing to their inherent particular principle of the input light polarization independence, and moreover the free spectral range (FSR) of the interference spectral is only decided by the length of the birefringence fiber used in the SI, which is easy to be adjusted. In principle, the fiber SI is constituted by inserting a section of birefringence fiber into the single mode fiber (SMF) loop. The birefringence fiber in the SI plays the role of introducing the optical path difference and causing the interference between the two counter-propagating waves in the Sagnac loop. Recently, with the development of the photonic crystal fiber (PCF), birefringence fiber based on PCF technology has been commercially available and widely applied in the SI based fiber torsion sensors. So far, various SIs constructed with different kinds of PCFs, including PM side-hole fiber [17], suspended twin-core fiber [18], side-Leakage PCF [19], highly birefringent-PCF with anisotropic microstructure [20] low-birefringence-PCF [21] and high birefringence asymmetric two-core PCF [22], have been proposed as the fiber torsion sensors. And yet, the fabrication of the PCF is complex and costly. Moreover, high-order modes easily excited at the splicing joints between the SMF and PCF increases the transmission loss. In addition, the splicing joints makes the sensor relatively fragile and a short service life, which are the barriers to their further large-scale applications.

To circumvent the aforementioned disadvantages of the PCF-SI based torsion sensor, a highly sensitive torsion sensor with femtosecond laser-induced low birefringence SMF-based Sagnac interferometer is proposed and experimentally demonstrated in this paper. A straight-line waveguide positioned horizontally with respect to the fiber core is inscribed by the femtosecond laser in the cladding of the SMF, which leads to the asymmetry stress distribution in the SMF, and then induces the low birefringence in the SMF. In this way, the low birefringence SMF in the fiber loop is fabricated and employed to construct the SI based torsion sensor. Compared with the PCF-SI based torsion sensor, there is no splicing joint in the SI, which lowers the transmission loss and makes the SI based torsion sensor more robust simultaneously. And then the responses of the proposed sensor with respect to torsion, temperature and strain are investigated, respectively. The device exhibits a torsion sensitivity of up to 1.2044 nm/degree. Meanwhile, the temperature cross-sensitivity and strain cross-sensitivity of the proposed torsion sensor are low to -0.00015 degree/ $^{\circ}\text{C}$ and 0.000037 degree/ μe , respectively. Moreover, theoretical analysis is carried out to compare with the experimental results to demonstrate the feasibility and good consistency.

2. Device fabrication

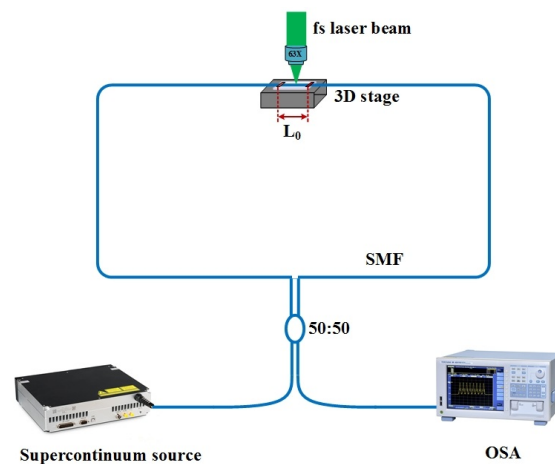


Fig. 1. Schematic configuration of the setup for the fabrication of low birefringence SMF-based Sagnac interferometer with femtosecond laser.

The schematic configuration of the setup for the fabrication of low birefringence SMF-based Sagnac interferometer with femtosecond laser is shown in Fig. 1. The fiber loop is composed of a 3-dB optical fiber coupler made by the conventional SMF. A supercontinuum source is connected to the input port of the fiber loop as the input source and an optical spectrum analyzer (OSA, Yokogawa AQ6370) with a resolution of 0.5 nm is connected to the output port of the fiber loop to real-timely monitor the transmission spectrum. A segment of SMF in the fiber loop is fixed on a computer controlled three-axis translating stage (Newport XML) by the fiber holders. The femtosecond laser beam emitted from the femtosecond laser at a center wavelength of 520 nm with a pulse duration of ~ 400 fs and a repetition rate of 200 kHz is focused into the cladding of the fixed SMF by using a $63 \times$ oil immersion lens. And the diameter of the focused spot is evaluated to be < 0.8 μm . To alleviate the distortion of the focal point introduced by the curved surface of the fiber, the objective and the fiber are both immersed into the index-matching oil.

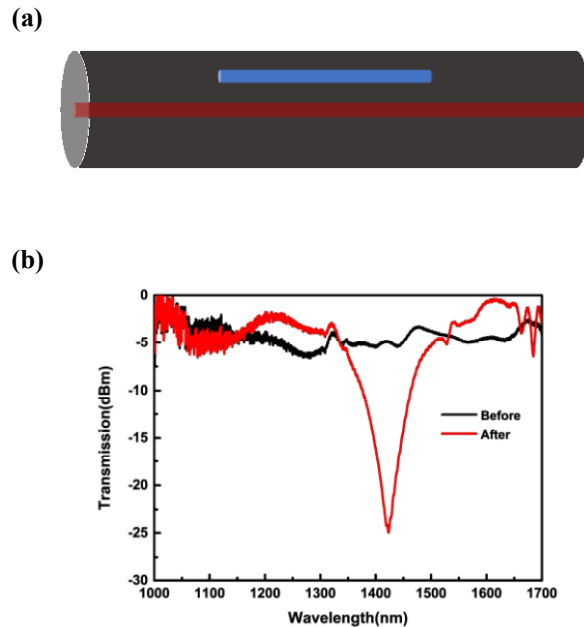


Fig. 2. (a) Schematic diagram of femtosecond laser inscribed straight-line waveguide in the SMF. (b) Measured normalized transmission spectrum of the SI before and after the fs laser processing.

The schematic diagram of femtosecond laser inscribed straight-line waveguide in the SMF is illustrated in Fig. 2(a). It is clearly seen that the straight-line waveguide is parallel to the fiber core with a separation of S . And the length of the straight-line waveguide is L_0 . According to Fernandes et al. [25], the femtosecond laser induced birefringence is a function of the separation S . To get a desired birefringence, the value of the separation S is set to 10 μm . The distance between the two fiber holders is only 10 cm. In view of protecting the objective and getting the maximal optical path difference, the length of the straight-line waveguide L_0 is set to 7 cm. In addition, the average pulse energy of the femtosecond laser is set to ~ 400 nJ. After designing the pattern of the straight-line waveguide in the computer, the fiber is moved automatically with respect to the focal spot of the fs-laser beam by the three-axis translating stage according to the designed pattern. And the scanning speed of the three-axis translating stage is set to 0.268 mm/s. When the straight-line waveguide is inscribed in the cladding of SMF, the stress distribution in the fiber becomes asymmetry, inducing the birefringence in the SMF [25-26]. And with the generation of the birefringence in the SMF, the optical path difference between the two counter-propagating waves in the fiber loop is introduced and cause interference when the two counter-propagating waves recombine at the

coupler. Figure 2(b) shows the measured normalized transmission spectrum of the SI in the wavelength range from 1000nm to 1700nm. From this figure, we can clearly see that there are small intensity fluctuations in the spectrum of the SI before the fs laser processing; however, after the fs laser processing, a large fringe dip at the wavelength of ~ 1420 nm with a fringe contrast of ~ 22 dB appears in the spectrum of the SI. This is attributed to the relatively low birefringence induced by the femtosecond laser inscribed straight-line waveguide and the limited length of the straight-line waveguide, which bring about a small optical path difference, resulting in the too large FSR. Meanwhile, it is worthy to note that the transmission loss is extremely low and the single fringe dip is adequate to fulfill the measurement of the torsion by utilizing the wavelength modulation. So we apply this femtosecond laser-induced low birefringence SMF-based Sagnac interferometer as a torsion sensor.

3. Experiment and results

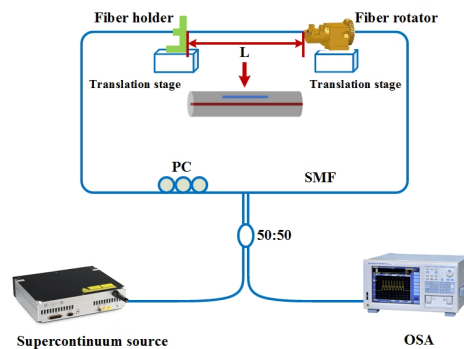


Fig. 3. Diagram of the experimental setup for torsion measurement.

In order to demonstrate its feasibility in fiber torsion sensing, the experimental setup, schematically illustrated in Fig. 3, is employed to investigate the torsion response of the proposed sensor. Another segment of SMF with the 7-cm-long femtosecond laser-induced low birefringence fiber positioned in the middle is fixed by a fiber holder on one side and a fiber rotator with an engraved dial on the other end. And the distance L between the fiber holder and the fiber rotator is 20 cm. The fiber holder and the fiber rotator are installed on two manual translation stages with the resolution of 0.02mm, respectively. In consideration of the measurement error induced by the bending effects, a small axial tension is applied to the fiber by pre-moving one translation stage to maintain it straight. A polarization controller (PC) is employed in the fiber loop to optimize the original interference spectral pattern. The input light from a supercontinuum source is launched into the fiber loop and the output is monitored by the optical spectrum analyzer.

To obtain the torsion response of the sensor, the torsion test is carried out by rotating the fiber rotator in the clockwise direction in the range from -120 to 360 degree with an increment of 10 degree, and the corresponding transmission spectra of the sensor are recorded by the optical spectrum analyzer, respectively. Figure 4(a) shows the transmission spectra of the sensor normalized with the spectrum of the supercontinuum under the torsion angle from 180 to 270 degree. To get clearly transmission spectra, the transmission spectra are smoothed using the Savitsky–Golay method, as shown in Fig. 4(b). From this figure, one can clearly see that the interference fringe is shifted towards shorter wavelength region as the applied torsion is increased from 180 to 270 degree in the clockwise direction. This is due to the fact that the torsion applied on the low birefringence SMF induces

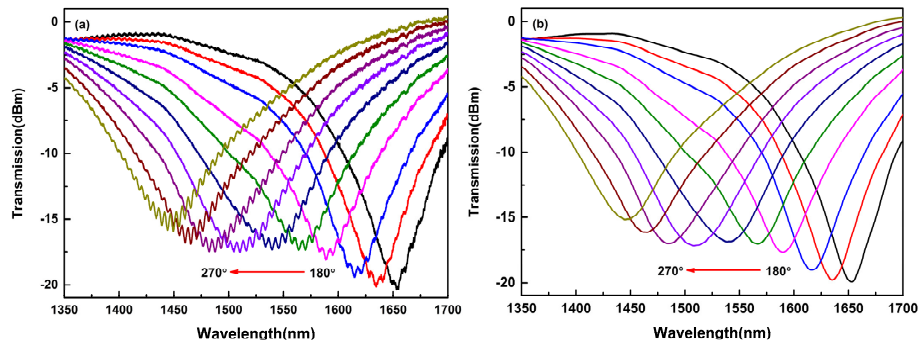


Fig. 4. (a) The transmission spectrum and (b) the smoothed transmission spectra of the sensor normalized with the spectrum of the supercontinuum under different applied torsions.

a circular birefringence, and the torsion-induced circular birefringence is related to the applied the torsion angle. When different torsion are applied on the fiber, the corresponding torsion-induced circular birefringence is different, which leads to the change of phase difference, and then resulting in the shift of the interference fringe. The relationship between the wavelength of the fringe dip and the applied torsion is plot in Fig. 5. As shown in Fig. 5, within a torsion range of -120 to 120 degree, the wavelength of the fringe dip shifts to the longer wavelength; while within a torsion range of 120 to 360 degree, the wavelength of the fringe dip shifts to the shorter wavelength. And the maximal wavelength variation is up to 390 nm. The

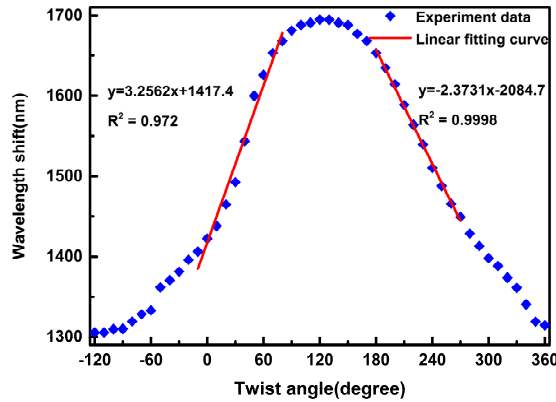


Fig. 5. Relationship between the wavelength variation of the fringe dip and the applied torsion.

Table 1. Torsion sensitivity of several special fibers based SI

SI structure	Wavelength sensitivity
Side-leakage photonic crystal fiber based SI [19]	0.9354 nm/degree
Highly birefringent photonic crystal fiber based SI [20]	~ 0.06 nm/degree
Low birefringence photonic crystal fiber based SI [21]	1 nm/degree
Polarization-maintaining elliptical core fiber based SI [23]	0.68 nm/degree
Microfiber based SI [24]	~ 0.9 nm/degree
femtosecond laser-induced low birefringence fiber based SI	3.2562 nm/degree

coefficients of the linear fitting curves in the torsion sensing range of -10 to 80 degree and 180 degree to 270 degree are 3.2562 and 2.3731 , corresponding to the torsion sensitivities of 3.2562 nm/degree and 2.3731 nm/degree, respectively. As the maximal wavelength resolution of the OSA employed in the experiment is 10 pm, a torsion resolution of 0.003 degree could be achieved during torsion measurement, which is actually quite high when taking into account the large measurement range. A variety of previously reported fiber optic torsion sensors that employed different special fibers based SI are presented in Table 1, where the achieved torsion sensitivity of the proposed sensor is comparable to the best result of the SI based torsion sensor reported so far.

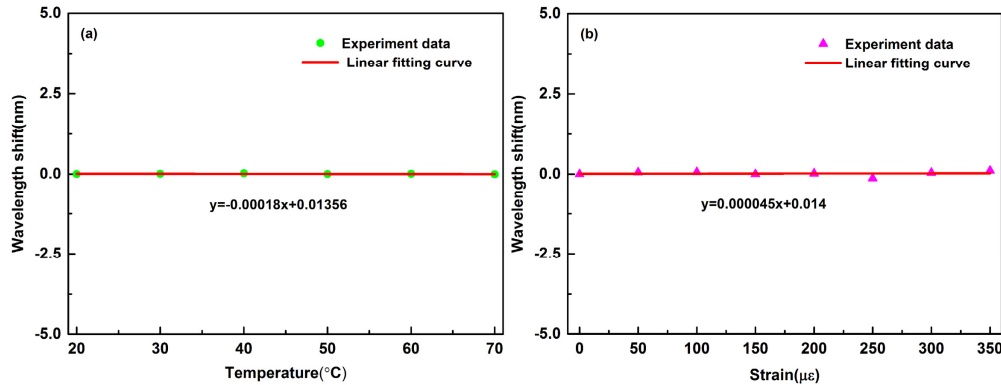


Fig. 6. (a) Temperature response and (b) Strain response of the proposed torsion sensor.

Experiments have also been performed to estimate the temperature cross-sensitivity of the proposed torsion sensor. The femtosecond laser induced low birefringence fiber is heated by a heating block, and the heating temperature is stepwise increased from 20 °C to 70 °C with an increment of 10 °C. After changing the temperature and before recording the corresponding transmission spectra, enough time (~ 10 min) is considered until the temperature is stable. Figure 6(a) shows the wavelength variation of the fringe dip with different temperature levels. It can be seen that the wavelength of the fringe dip hardly changes. The coefficient of the linear fitting curves in the temperature sensing range of 20 °C to 70 °C is -0.00018 , corresponding to the temperature cross-sensitivity of -0.000055 degree/°C. The last point we have investigated is the strain cross-sensitivity of this torsion sensor. As aforementioned, the fiber holder and the fiber rotator employed to fix the 20 cm long test fiber are installed on two manual translation stages with the resolution of 0.02 mm, respectively. So the strain test within the range from 0 to 350 $\mu\epsilon$ with a step of 50 $\mu\epsilon$ is implemented by means of moving one translation stage to stretch the test fiber along the fiber axis, and the corresponding wavelength variation of the fringe dip with different temperature levels are shown in Fig. 6(b). The obtained strain sensitivity of this torsion sensor is only 0.000045 nm/ $\mu\epsilon$, corresponding to the strain cross-sensitivity of 0.000013 degree/ $\mu\epsilon$. The obtained experimental results above vividly confirm that the proposed torsion sensor is immune to temperature and strain. This can be readily explained by the fact that the low birefringence is introduced by the femtosecond laser inscribed straight-line waveguide in the fiber cladding, which almost has the same thermo-optic coefficient and elasto-optical coefficient as the fiber. When the temperature and the axial strain are applied onto the test fiber uniformly, the corresponding refractive index variation induced by the thermo-optic effect and elasto-optical effect along the two perpendicular directions of the fiber are almost the same, resulting in that the birefringence remains the same. As there is no variation in the birefringence, the wavelength of the fringe dip hardly changes, so the proposed torsion sensor is insensitive to the temperature and strain simultaneously, which is confirmed in the experiment.

4. Analysis and discussion

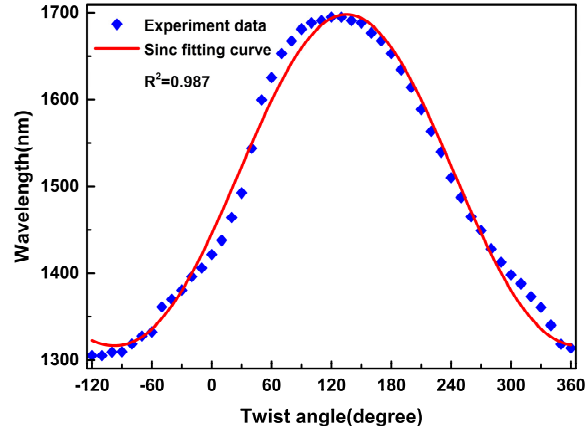


Fig. 7. Comparison between the experiment result (blue rhombus) and the Sinc fitting result (red line).

Considering the asymmetry stress distribution introduced by the femtosecond laser-inscribed straight-line waveguide and the deviation from a circular shape of the fiber core, the test fiber can be regarded as a fiber with an intrinsic linear birefringence B . For the test fiber under torsion, a circular birefringence will be induced by the shear strain and is dominant for the total birefringence [27]. So the total effects of the twisted fiber can be treated as a retarder and a rotator [28]. And the retardance $\Delta\Phi$ caused by the applied torsion between the two orthogonal guided polarization modes is a function of twist rate ω and twist length L , which can be described as [28]:

$$\Delta\Phi = 2 \sin^{-1} \left(\frac{\rho}{\sqrt{1+\rho^2}} \sin \gamma L \right) \quad (1)$$

where

$$\rho = \frac{\Delta\beta}{2(\omega - \alpha)} \quad (2)$$

$$\gamma = \frac{1}{2} \sqrt{\Delta\beta^2 + 4(\omega - \alpha)^2} \quad (3)$$

where $\Delta\beta$ refers to the intrinsic propagation constant retardance between the two polarizations. And α is the optical rotation introduced by the photo-elastic effect, which is given by:

$$\alpha = g\omega \quad (4)$$

Here, the proportionality constant g is a constant determined by the photo-elastic coefficients of the material. In the case of the SMF, the value of the g is 0.08.

In view of the low birefringence in the test fiber, the torsion applied on the test fiber is regarded as a strong twist. In the case of a fiber under a strong twist, the total birefringence is dominated by the induced circular birefringence [6, 27]. So the Eq. (1) can be simplified as [6,21]:

$$\Delta\Phi = \Delta\beta \frac{\sin[(\omega - \alpha)L]}{\omega - \alpha} \quad (5)$$

Accordingly, the torsion induced birefringence can be described as [6]:

$$\Delta B = B \frac{\sin[(\omega - \alpha)L]}{\omega - \alpha} \quad (6)$$

For the birefringence fiber based SI, the normalized transmittance ratio T of the light is:

$$T = \frac{1}{2}(1 - \cos \Phi) \quad (7)$$

Here, $\Phi = 2\pi BL/\lambda$ is the initial phase difference. The min transmission occurs when the $\Phi = 2m\pi$ ($m = 0, 1, 2, \dots$). Then, the wavelength for the fringe dip can be expressed as:

$$\lambda_{dip} = BL / m \quad (8)$$

Consequently, the wavelength variation $\Delta\lambda$ of the fringe dip is given by:

$$\Delta\lambda = \Delta BL / m \quad (9)$$

According to the Eqs. (6), (8) and (9), for the case of the low birefringence fiber in the SI under torsion, the wavelength variation $\Delta\lambda$ of the fringe dip in terms of the torsion can be expressed as:

$$\Delta\lambda = \frac{\sin[(\omega - \alpha)L]}{\omega - \alpha} \lambda_{dip} \quad (10)$$

From the Eq. (10), we can clearly see that the wavelength variation $\Delta\lambda$ of the fringe dip is following a pattern of Sinc function with the torsion. Then we use a Sinc function to fit the obtained experiment data, as shown in Fig. 7. It is obvious that the wavelength variation $\Delta\lambda$ changes with the applied torsion angle as a Sinc function, which agrees well with the theoretical analysis, vividly confirming the viability of the proposed torsion sensor.

5. Conclusions

In summary, a high sensitivity torsion sensor with femtosecond laser-induced low birefringence SMF-based SI has been proposed and experimentally demonstrated in this paper. The low birefringence SMF is fabricated by simply inscribing a straight-line waveguide in the cladding and positioned horizontally with respect to the fiber core with the femtosecond laser. With the inscription of the straight-line waveguide in the cladding, the stress distribution in the SMF changes into asymmetry, giving rise to the low birefringence. Unlike most of the previous reported SI based torsion sensors, the low birefringence is directly fabricated by femtosecond laser in the fiber loop, so there is no splicing joint in the SI, which lowers the transmission loss and makes the SI based torsion sensor more robust simultaneously. It is observed that the wavelength of the fringe dip is very sensitive to torsion. The experiment result shows that the proposed torsion sensor exhibits a torsion sensitivity of up to 3.2562 nm/degree, with the high torsion resolution of 0.003 degree. In contrast, the temperature cross-sensitivity and strain cross-sensitivity of the proposed torsion sensor are low to -0.000055 degree/ $^{\circ}\text{C}$ and 0.000013 degree/ μe , respectively, thus overcoming the cross-sensitivity problem resulting from temperature and strain. Moreover, theoretical analysis is carried out to compare with the experimental results to demonstrate the feasibility and good consistency. The proposed torsion sensor with the prominent advantages such as extremely simple and robust, low loss and immunity to temperature and strain cross sensitivity effects is highly desirable for modern smart structure monitoring applications.

Funding

National Natural Science Foundation of China (NSFC) (61775074); National 1000 Young Talents Program, China.